Materials and Design 116 (2017) 504–514

Contents lists available at ScienceDirect

Materials and Design

journal homepage: www.elsevier.com/locate/matdes

Finite element modeling of spark plasma sintering: Application to the reduction of temperature inhomogeneities, case of alumina

Youssef Achenani [a,*], Malika Saâdaoui [a,*], Abdelkhalek Cheddadi [a], Guillaume Bonnefont [b], Gilbert Fantozzi [b]

[a] Mohammed V University in Rabat, Mohammadia School of Engineers, P.O. Box 765, Agdal, Rabat, Morocco
[b] Lyon University, MATEIS, UMR 5510 CNRS, National Institute of Applied Sciences of Lyon, Avenue Jean Capelle, F-69621 Villeurbanne Cedex, France

ARTICLE INFO

Article history:
Received 2 August 2016
Received in revised form 16 December 2016
Accepted 19 December 2016
Available online 21 December 2016

Keywords:
Spark plasma sintering
Finite element modeling
Temperature distribution
Die location
Die insulation

ABSTRACT

Increasing attention is being paid to numerical modeling of spark plasma sintering (SPS) due to its significant importance for the comprehension and the optimization of this process. In this study, SPS sintering experiments of alumina were performed and their results were used to develop faithful simulations of the temperature distribution, based on a thermal-electrical finite element model. Particular focus was put on the axial temperature distribution within the sample, rarely considered in the literature. The model was used to analyze the influence of various experimental parameters potentially affecting the temperature distribution (axial asymmetry, die location and insulation) and simple methods, based on the die location and its insulation, are proposed to reduce the temperature inhomogeneities in the sample.

1. Introduction

Spark Plasma Sintering (SPS) is a consolidation process based on Joule heating by the application of a pulsed electrical current to a graphite die containing the material powder. Compared to other conventional sintering methods, SPS offers exceptional benefits, including rapid heating rate and reduced sintering temperature and holding time, which allow to avoid grain growth and to improve mechanical or physical properties of the final products. So that, increasing attention is paid to this technique, which has been applied to a variety of advanced materials in a wide range of application fields [1–3].

The sample temperature is of particular importance to the SPS process, since it determines the structure and properties of the material and their homogeneity. However, it is difficult to control due to inherent experimental difficulties and the large number of the involved parameters. In recent years, finite element modeling with consideration of the coupled phenomena involved during SPS sintering played a crucial role in understanding this process. Most of the models considered thermoelectric coupling [4–7] to determine electrical and temperature fields. Some works integrated mechanical coupling to investigate stress distribution as in [8–12], or a densification model [13–18].

A complex temperature distribution within the tools and the sample has been evidenced, with temperature gradients depending on process parameters such as the heating rate [15,19–21], geometrical aspects of the sample and tools [6,7,15,18,22] and thermophysical parameters, especially material conductivity [3,10,22,23]. A parametric analysis of Muñoz et al. [21] highlighted the difficulty to predict the effect of one parameter independently of the others. However, most of the numerical studies lack of experimental validation and their accuracy depend on the simplifying assumptions related to the device parts taken into account, power or heating conditions, and contact resistances between the graphite tools and between the punches and the sample. Anselmi-Tamburini et al. [24] and Cincotti et al. [25] highlighted the importance of considering the RMS (Root Mean Squared) value of the pulsed current input to determine the Joule effects. Whereas the first simulations considered a constant applied electric potential or current, Muñoz and Anselmi-Tamburini [10] and Wang et al. [15] introduced a Proportional-Integral-Differential (PID) module for better reproduction of the experimental thermal sintering cycle. Moreover, the contact resistances have often been neglected in numerical modeling. Few authors developed calibration or experimental methods to determine them [14,26–30]. Vertical contact resistances are much larger than horizontal ones [14,26,27] and the influence of the applied pressure has been outlined in [24,29,31,32].

In general, symmetrical thermal boundary conditions are used and the axial temperature distribution within the sample has been barely investigated. In this study, standard sintering experiments were performed with alumina, chosen as a model for non-conductive materials, and their results were used to develop faithful simulations with limited approximations. The influence of various experimental parameters on both radial and axial temperature distributions was then investigated, and simple methods based on the die location and its

* Corresponding authors.
E-mail addresses: achenaniyoussef@yahoo.fr (Y. Achenani), saadaoui@emi.ac.ma (M. Saâdaoui).

http://dx.doi.org/10.1016/j.matdes.2016.12.054

insulation are proposed to reduce temperature inhomogeneities in the sample.

2. Procedure and modeling

2.1. SPS experiments and temperature measurements

Standard sintering experiments have been performed with an ultra-pure alumina (BMA-15 Baikowski, >99.99%), using an HP D25/1 FCT SPS equipment (FCT Systeme GmbH, Germany) configuration of which is shown in Fig. 1. It includes a graphite die (with thickness of 10 mm and height of 48 mm) containing the sample, two punches (with a height of 35 mm and the same diameter as the sample) protected by conical spacers (large diameter of 80 mm) and two water-cooled electrodes located at the upper and lower ends of the apparatus. A central hole of diameter 10 mm is drilled in each element for temperature measurements. The sintering experiments were performed in a temperature-control mode using an optical pyrometer focused on the upper graphite punch (position A), at 4 mm from the sample, and a PID controller that allow to adjust the electric current automatically. The temperature was also systematically controlled at three other positions of the system (Fig. 1): An optical pyrometer focused in a hole (3 mm diameter) drilled in the middle of the die, measured the temperature, T_B, at 3 mm from the sample (position B) and two K-type thermocouples measured the temperatures T_{S_1} and T_{S_2} of the upper and lower spacers, at positions S_1 and S_2 respectively. The experimental thermal cycle consisted of a rise in temperature at 100 °C/min up to 1300 °C with a dwell time of 10 min, during which a constant pressure of 73 MPa was applied to the sample. The following pulse sequence was chosen: 10 ms of pulsed current followed by 5 ms of current without pulse. Graphite foils (Papyex® Mersen) of 0.4 mm thickness were used as interfaces (Fig. 1) and a set of experiments was performed using felt thermal insulator (Mersen) around the die. The samples were processed with a final thickness of 2.5 mm and two different diameters, 20 and 40 mm.

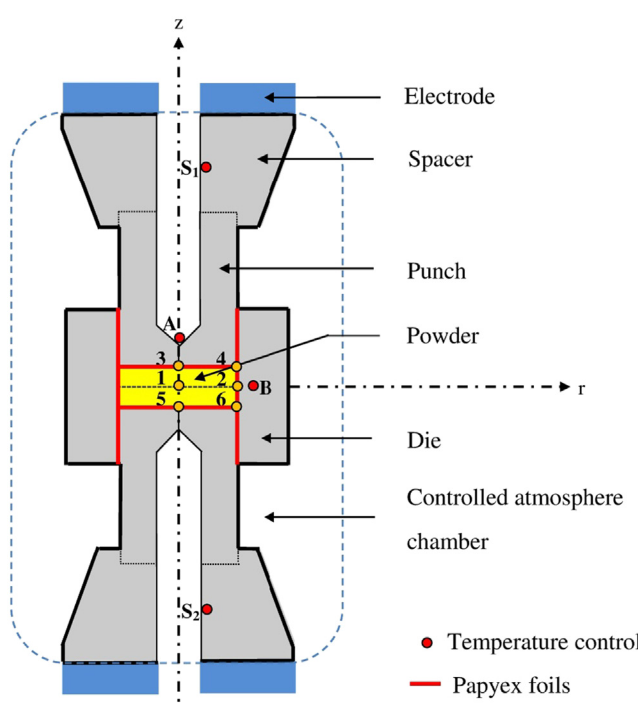

Fig. 1. Illustration of the SPS configuration with locations of the temperature measurements (points A, B, S_1 and S_2) and reference locations in the sample (points 1 to 6).

Table 1
Parameters of the study. The bold letters correspond to the conditions of the performed experiments.

Parameters	Investigated range
Sample dimensions (mm)	
Diameter, ϕ	**20**, **40**
Thickness, th	**2.5**, 5, 10
Thermal insulation of the die	**Without**, **total**, partial
Location of the die relative to the sample	**Centered**
	Off-centered 1 to 3 mm downward
	Off-centered 1 to 3 mm upward

2.2. Numerical modeling

Finite element modeling was performed using COMSOL Multiphysics® to simulate the thermoelectric coupling during SPS sintering, governed by the equations of energy and electric charge conservation. We considered the system between the spacers ends and due to the axisymmetrical configuration, the calculations were limited to only one-half of its section, where the temperature, T(r, z, t), is given as a function of time, t, in the cylindrical coordinates (r, z) by:

$$\rho c_p \frac{\partial T}{\partial t} = \frac{1}{r}\frac{\partial}{\partial r}\left(r k_r \frac{\partial T}{\partial r}\right) + \frac{1}{z}\frac{\partial}{\partial z}\left(r k_z \frac{\partial T}{\partial z}\right) + \dot{q}_i \tag{1}$$

where ρ, c_p, k_r and k_z, represent respectively the density, the specific

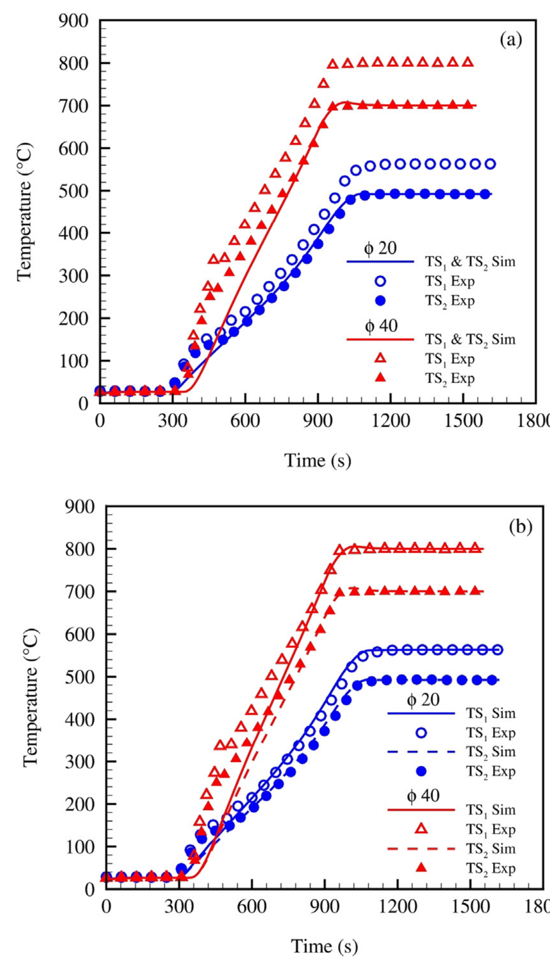

Fig. 2. Comparison of experimental (Exp) and simulated (Sim) temperatures at the top (T_{S_1}) and bottom (T_{S_2}) spacers for symmetrical (a) and asymmetrical (b) thermal boundary conditions.